doi:10.20944/preprints202001.0035.v1

Peer-reviewed version available at *Entropy* **2020**, *22*, 251; doi:10.3390/e22020251

*Article*

# Self-Propulsion Promotes Polymerization

**Maximino Aldana** [1,2,†,*], **Miguel Fuentes-Cabrera** [3,4,†] and **Martín Zumaya** [1,2,†]

1. Instituto de Ciencias Físicas, Universidad Nacional Autónoma de México. Avenida Universidad s/n, Colonia Chamilpa. Código Postal 62210. Cuernavaca, Morelos, México.
2. Centro de Ciencias de la Complejidad, Universidad Nacional Autónoma de México. Ciudad de México, México.
3. Center for Nanophase Materials Sciences, Oak Ridge National Laboratory. Oak Ridge, TN, United States of America.
4. Computational Sciences and Engineering Division, Oak Ridge National Laboratory. Oak Ridge, TN, United States of America.

* Correspondence: max@icf.unam.mx; Tel.: +52-777-329-1787

† All authors contributed equally to this work. Their names appear in alphabetic order.

**Abstract:** Self-assembly is a spontaneous process through which macroscopic structures are formed from basic microscopic constituents (e.g. molecules or colloids). By contrast, the formation of large biological molecules inside the cell (such as proteins or nucleic acids) is a process more akin to self-organization than to self-assembly, as it requires a constant supply of external energy. Recent studies have tried to merge self-assembly with self-organization by analyzing the assembly of self-propelled (or active) colloid-like particles whose motion is driven by a permanent source of energy. Here we present evidence that points to the fact that self-propulsion considerably enhances the assembly of polymers: self-propelled molecules are found to assemble into polymer-like structures, the average length of which increases towards a maximum as the self-propulsion force increases. Beyond this maximum, the average polymer length decreases due to the competition between bonding energy and disruptive forces that result from collisions. The assembly of active molecules might have promoted the formation of large pre-biotic polymers that could be the precursors of the informational polymers we observe nowadays.

**Keywords:** self-assembly; self-propulsion; self-organization; polymerization

---

## 1. Introduction

The formation of long biological polymers inside the cell (e.g. proteins and nucleic acids) is an out of equilibrium process that is carried out by a molecular machinery which, nowadays, is extremely complex. Such complexity is expected to have emerged gradually during the early stages of the origin of life [1,2]. However, even within a primitive scenario, it is still unclear what were the mechanisms that lead to the polymerization of large biological molecules from small monomers [3–7]. Recent work have shown that the assembly of large biological structures is considerably enhanced if it occurs far from equilibrium [8,9]. Two ways of introducing non-equilibrium conditions have been studied so far. The first one considers assembly in the presence of thermal gradients [8,9]. The second allows molecules to constantly move in a self-propelled manner due to the continuous supply of external energy [10,11]. The latter has been termed *active-* or *dynamic self-assembly*, and it is believed to have played an important role in the formation of large biological molecules from smaller constituents in pre-biotic Earth [12].

In this work we consider a model of active self-assembly in which self-propelled molecules, represented as a polygons, (see Figure 2), move in a thermal bath at temperature $T$. The polygonal

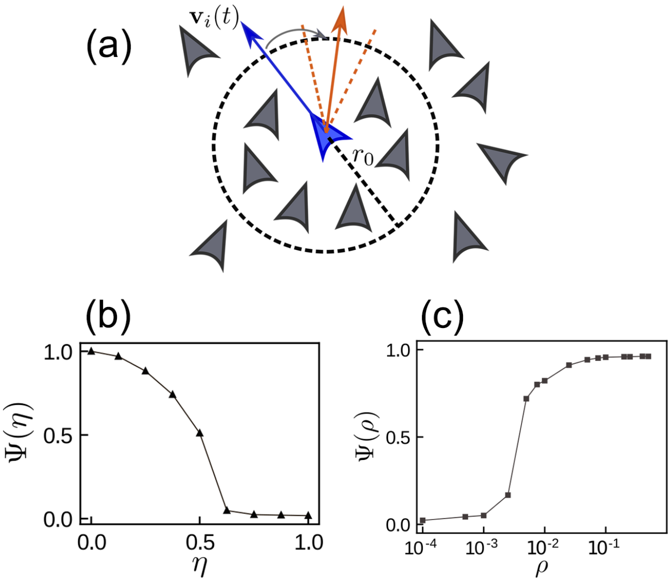

**Figure 1.** Vicsek Model of Collective Motion. **(a)** Particles in the system interact through alignment interactions, where each particle tries to match its own direction of motion with the average direction of all others inside a circular neighborhood of radius $r_0$, plus some noise. The model exhibits an order-disorder phase transition either as a function of the noise intensity $\eta$, while keeping the particle density $\rho$ fixed **(b)**, or as a function of $\rho$, while keeping $\eta$ constant **(c)**. The order parameter $\Psi$, which is the magnitude of the average velocity of the entire system, acquires the value $\Psi \approx 0$ in the disordered phase, where the particles move in uncorrelated random directions, and $\Psi \approx 1$ in the ordered phase, where all the particles in the system move in a common direction.

shape is inspired by the shape of natural and unnatural DNA/RNA bases, which are know to form a variety of hydrogen bonded structures in equilibrium conditions. Further, when DNA/RNA bases and nucleosides are deposited on substrates, they are known to align along features of the substrates which, acting as sinks, attract molecules and promote the formation of chain-like structures [13–17]. We do not consider the effect of a substrate, but focus instead on studying how self-propelled molecules might assemble in non-equilibrium conditions. In this scenario, we assume that two molecules can either repel or bind, depending on the angle of the collision. The interaction between the molecules is defined through Lennard-Jones potentials, and the attractive and repulsive interactions are tuned by different cut-offs.

Numerical simulations clearly show that self-propulsion considerably improves the assembly of polymers, somewhat in agreement with previous related studies [10,11]. (Unlike Ref. [10,11], which considers only the formation of two dimensional structures, here we we explicitly consider the formation of linear polymers.) Before proceeding to present the model used here and the results it produces, it is convenient to explain the differences between self-assembly and self-organization. We do this in the following section.

## 2. Self-propulsion, self-assembly and self-organization

Self-assembly is a spontaneous process that takes place in equilibrium, where small dissociated blocks minimize the free energy of the system by forming macroscopic organized structures. This is the same process by which salt crystals, lipid membranes and other structures are formed [18–21]. Self-assembly is characterized by the fact that the dissociated blocks (molecules, colloids, etc.) move and bind together in equilibrium in a thermal bath at constant temperature $T$. They perform Brownian motion and are driven solely by the effect of temperature. The thermal motion leads to collisions, and the combination of attraction and repulsion (from collisions) results in the spontaneous formation of a

Peer-reviewed version available at Entropy 2020, 22, 251; doi:10.3390/e22020251

variety of structures. *Self-assembly* is fundamentally different to *self-organization* [8,22]. Self-organization requires a constant supply of external energy into the system for the constituent dissociated blocks to organize into ordered structures. Self-organized systems are, by definition, far from thermodynamic equilibrium and driven by external forces, not just by thermal motion.

Self-organization is prevalent at many scales in biology. Consider, for instance, the formation of macromolecules such as proteins, nucleic acids or ribosomes, inside the cell: all of them require the constant input of energy (via nutrients that are converted into ATP, GDP or enzymes). At a larger scale, self-organization is observed in the motion of flocks of birds, fish swarms and bacterial colonies, to name a few [23,24]. At such scales, the constituent blocks (bird, fish, bacterium) are driven by the constant energy influx obtained from the intake of nutrients. It is apparent that the formation of structures in biology requires self-organization, not just self-assembly. It remains to be seen whether self-organization played a role in pre-biotic chemistry, e.g. in the formation of primordial informational oligomers. However, given the current prevalence of self-organization in biology, it seems reasonable to include non-equilibrium scenarios when investigating pre-biotic routes to macromolecular formation [5,25].

A first step to address this problem is to consider the assembly of self-propelled particles [11]. Systems of interacting self-propelled particles have been extensively studied [23,26], starting with the seminal paper by Vicsek et.al [26], where the so called Vicsek model of collective motion was introduced. In this model, self-propulsion consists in the motion of particles that maintain a constant speed, regardless of the interactions and forces acting on them. In the Vicsek model for a flock of birds, each bird moves with a constant speed, even when it interacts with other birds in the flock. These interactions only change the direction of motion of the bird, but not its speed. It is assumed that the energy necessary for each bird to sustain a constant speed is provided by its metabolism, i.e. the food each bird has to eat in order to be alive, move and fly. Ultimately, this food is an external source of energy that keeps the bird moving for long periods of time. The Vicsek model can be applied to any particle in general, not just birds, and each particle moves in the average direction of motion of the particles within a local neighborhood of radius $r_0$. To this average direction of motion, a white uncorrelated noise of amplitude $\eta$ is added (Figure 1a). Vicsek's model exhibits an order-disorder phase transition driven either by the noise intensity in the system (Figure 1b), for a fixed particle density $\rho$, or by the local density $\rho$, for a fixed noise intensity (Figure 1c). In the ordered phase, the system displays coherent motion, where all the particles move approximately in the same direction; in the disordered phase, particles move in random uncorrelated directions (like Brownian particles). One of the virtues of the Vicsek model is that simple local interaction rules can give rise to collective organized behavior in many-particle systems out of equilibrium.

While self-propulsion makes sense for birds, fish and bacteria, its applicability to molecules is not completely justified. Nonetheless, there are experimental studies that have managed to include propulsion in molecular systems. One of the most significant ones is that of Bausch's group [27,28]. This group has deposited micron size filaments on a substrate that was decorated with molecular motors. The motors threaded and subsequently pushed the filaments, providing a source of constant motion. The filaments were labeled with fluorophores, and their collective movement imaged. By changing the density, Bausch's group revealed the formation of mesmerizing dynamic structures, e.g. vortices, moving clusters and moving bands, that have been considered and observed in previous studies.

Others have recognized that self-propulsion may have played an important role in the formation of pre-biotic molecules [12]. For instance, [11] showed that self-propelled colloids assemble faster and form larger structures than colloids without self-propulsion. Along the same lines, the formation of protein domains on the surface of the cell membrane was analyzed under two scenarios [8]. In the first scenario, the proteins interact, via electrostatic forces, with the phospholipids of the membrane. These forces drive the spontaneous assembly of the proteins through equilibrium processes, with the consequent formation of protein domains on the cell membrane. In the second scenario,

Peer-reviewed version available at Entropy 2020, 22, 251; doi:10.3390/e22020251

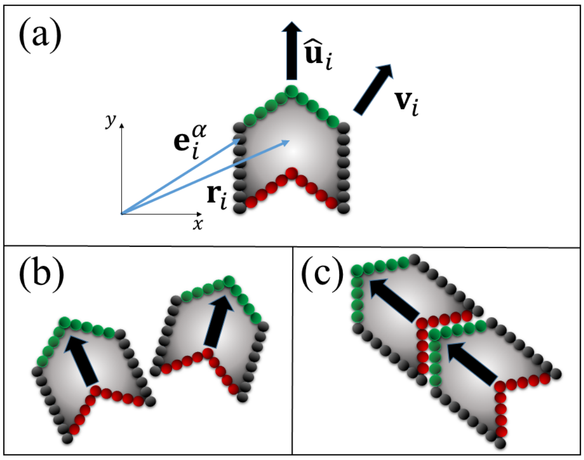

**Figure 2.** **(a)** Schematic representation of the basic rigid molecule. The sides of the molecule are discretized into spherical subunits with positions $\mathbf{e}_i^\alpha$ which exert attractive or repulsive forces on the spherical subunits of other molecules. The entire molecule is characterized by the position $\mathbf{r}_i$ of the center of mass, its velocity $\mathbf{v}_i$ and orientation $\hat{\mathbf{u}}_i$. Note that the velocity and orientation are not necessarily parallel. The self-propulsion force always acts in the direction of the orientation vector $\hat{\mathbf{u}}_i$. The edges of the molecule are colored according to the repulsive or attractive forces they exert on other molecules: if two molecules collide through edges of the same color, the force is repulsive as in **(b)**, whereas the force is attractive only between the green and red edges, as in **(c)**. The dynamics take place on a 2D-space.

the proteins, which are assumed to be close to the membrane, are out of equilibrium due to a phosphorylation-dephosphorylation cycle driven by ATP. The formation of protein domains on the cell membrane is also observed, however, these domains are considerably larger (about four hundred times fold) than those formed via equilibrium processes. These results show that the external input of energy, via self-propulsion or other sources (such as ATP), can considerably enhance the assembly of structures. To the best of our knowledge, formation of DNA-like polymers in non-equilibrium scenarios have not been considered yet. It's very well known, however, that DNA-like bases deposited on substrates do form a variety of substrates, some of them linear, but all these studies have taken equilibrium conditions into account [13–17].

Here we take a first step towards investigating how self-propelled monomers might form polymeric-like structures in the absence of a substrate. For this we borrow ideas from recent studies where the assembly of self-propelled molecules or colloids was investigated [10,11,25,29,30]. In these studies, dissociated blocks were placed in a thermal bath at temperature $T$, and in addition to performing Brownian motion, they are thought to be able to transform energy from its surrounding into directed motion. The combination of repulsive and attractive interactions, as well as geometry, symmetry and direction of motion, lead to emergent collective behavior, such as collective motion, jamming, motility induced phase separation and the assembly of structures. An interesting example of this type of systems is the one presented in [29], where different organisms are modeled as self-propelled colloids composed of a collection of rigid spherical subunits. In the next section, we show how a model that borrows some of these ideas can be used to study polymer formation from a collection of self-propelled monomers.

## 3. Model Definition

Recent studies have shown that steric interactions and geometry are relevant for the emergence of different kinds of collective behavior in systems of self-propelled colloids. Rigid molecules should act in a similar manner, their steric interactions and geometry causing blockages that prevent motion. Therefore, for rigid molecules, the usual assumption of constant speed seems not longer adequate.

Peer-reviewed version available at Entropy 2020, 22, 251; doi:10.3390/e22020251

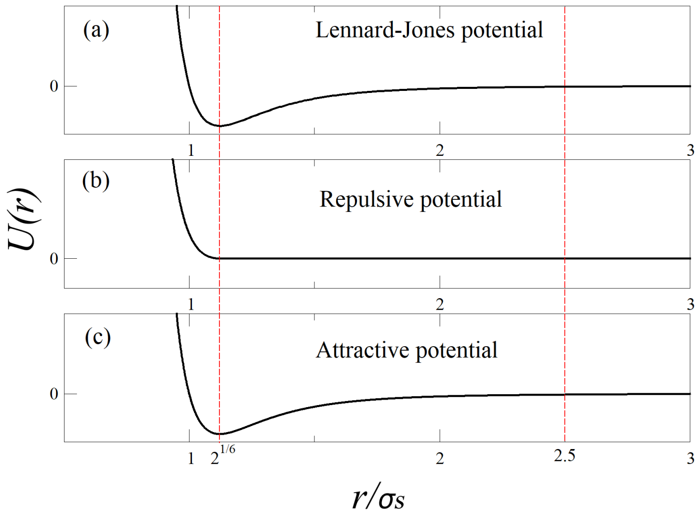

**Figure 3.** Interaction potentials used in the numerical simulations. **(a)** Lennard-Jones potential given in Eq. 1. **(b)** Repulsive potential obtained from the Lennard-Jones potential by setting the cut-off distance $r_c = 2^{1/6}\sigma_\text{S}$. **(c)** Attractive potential obtained by setting the cut-off distance $r_c = 2.5\sigma_\text{S}$. The dashed lines indicate the cutoff distances for the repulsive and attractive potentials.

Instead, it is seems more adequate to assume a constant self-propulsion force acting on each rigid molecule. This requires the magnitude and direction of the velocity of each molecule to be modified according to the interactions it has with other molecules in the system.

Our model consists of $N$ active rigid molecules $\{1, 2, \ldots, N\}$ characterized by the position of their center of mass $\mathbf{r}_i$, velocity $\mathbf{v}_i$ and orientation $\hat{\mathbf{u}}_i = (\cos\theta_i, \sin\theta_i)$. Following Wensink and Löwen [31], and Mallory [11], the sides of each molecule are discretized into $M$ spherical subunits of radius $\sigma_\text{S}$ and positions $\mathbf{e}_i^\alpha$, where the superscript refers to the $\alpha$-th subunit, and the subscript refers to the $i$-th parent molecule (see Figure 2a). Subunits within the same molecule do not interact with each other, however, subunits of different molecules interact through Lennard-Jones potentials of the form

$$U(e_{ij}^{\alpha\beta}) = 4\epsilon\left[\left(\frac{\sigma_\text{S}}{e_{ij}^{\alpha\beta}}\right)^{12} - \left(\frac{\sigma_\text{S}}{e_{ij}^{\alpha\beta}}\right)^{6}\right] \tag{1}$$

where $\mathbf{e}_{ij}^{\alpha\beta} = \mathbf{e}_i^\alpha - \mathbf{e}_j^\beta$, is the relative distance between the $\alpha$-th subunit of the $i$-th molecule and the $\beta$-th subunit of the $j$-th molecule. The total interaction potential $U_{ij}$ between the $i$-th and the $j$-th molecules is given by

$$U_{ij} = \sum_{\alpha,\beta} U(e_{ij}^{\alpha\beta}). \tag{2}$$

We consider a *dry* scenario, and therefore hydrodynamic interactions between molecules and the surrounding media are not taken into account. The dynamics of the system take place on a 2D-plane and evolve according to the following pair of coupled over damped Langevin equations for the translational and rotational motion of each molecule:

$$\frac{\partial \mathbf{r}_i}{\partial t} = -\frac{1}{\gamma_t}\sum_{i\neq j}\nabla_{\mathbf{r}_i}U_{ij} + F_\text{sp}\hat{\mathbf{u}}_i + \sqrt{2\gamma_t^2 D}\boldsymbol{\xi}_i^t(t), \tag{3a}$$

$$\frac{\partial \theta_i}{\partial t} = -\frac{1}{\gamma_r}\sum_{j\neq i}\nabla_{\theta_i}U_{ij} + \sqrt{2D_r}\xi_i^r(t), \tag{3b}$$

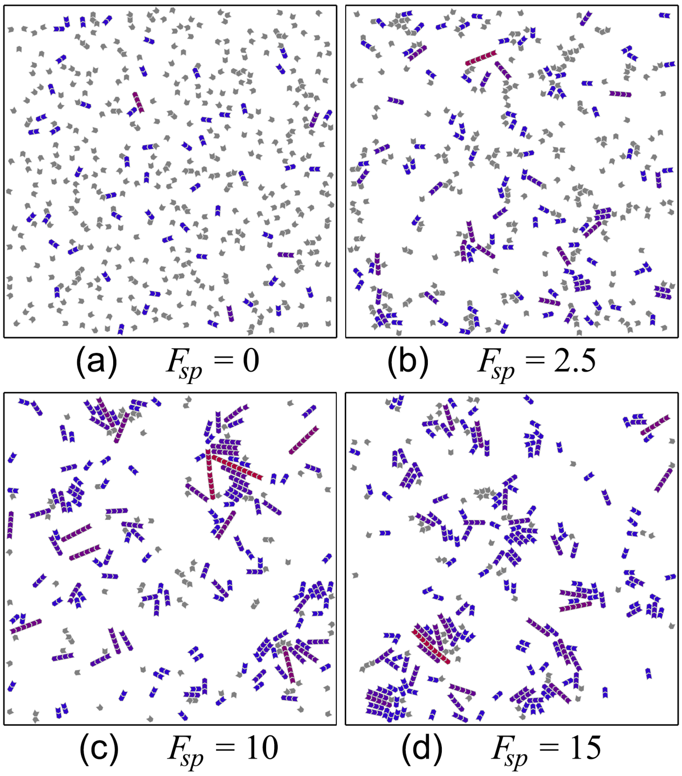
(a) $F_{sp} = 0$ (b) $F_{sp} = 2.5$

(c) $F_{sp} = 10$ (d) $F_{sp} = 15$

**Figure 4.** Snapshots of the system with fully periodic boundary conditions showing the effect of self-propulsion on the assembly of molecules. Different snapshots correspond to different values of the self-propulsion force $F_{sp}$. In all cases the temperature is $T = 0.1$. Note that with no self-propulsion (panel **(a)**, $F_{\text{sp}} = 0$), only very small chains are formed. This case would correspond to spontaneous self-assembly. As the self-propulsion force $F_{sp}$ increases, longer chains appear. It is apparent that self-propulsion considerably improves the assembly of molecules as compared to spontaneous self-assembly.

where $\gamma_t$ and $\gamma_r$ are the translational and rotational friction coefficients, $F_{\text{sp}}$ is the self-propulsion force, and $D$ y $D_r$ are the translational and rotational diffusion coefficients. $\boldsymbol{\xi}^t$ and $\xi^r$ are Gaussian white noise terms for both the translational and rotational motion, and are given by $\langle \boldsymbol{\xi}_i^t(t) \rangle = 0$, $\langle \boldsymbol{\xi}_i^t(t) \cdot \boldsymbol{\xi}_j^t(t') \rangle = \delta_{ij}\delta(t - t')$, $\langle \xi_i^r(t) \rangle = 0$ and $\langle \xi_i^r(t)\xi_j^r(t') \rangle = \delta_{ij}\delta(t - t')$.

Forces between molecules are obtained from the gradient of the interaction potential, $\nabla_{\mathbf{r}_i} U_{ij}$, and the torques generated by these forces are obtained by differentiating the interaction potential with respect to their direction of motion $\theta_i$, i.e. $\nabla_\theta U_{ij}$. Eqs. (3) describe the motion of the center of mass (COM) and orientation of each molecule. All the spherical subunits within a molecule move and rotate rigidly with respect to the COM.

Interactions between the subunits in separate molecules can be either attractive or repulsive, depending on which side of the molecule they are located (see Figure 2b). Different cut-off distances, $r_c$, ensure that the interaction potential given by Eq. (1) becomes zero when the two spherical subunits are separated by a distance larger than $r_c$ (see Figure 3). In the case of repulsive interactions, the cut-off distance is set to $r_c = 2^{1/6}\sigma_{\text{s}}$ (Figure 3b); for the attractive case, $r_c = 2.5\sigma_{\text{s}}$ (Figure 3c). In both cases, the potential is shifted after truncation so that $V(r_c) = 0$.

The geometry chosen for each molecule (Figure 2a) and the definition of the attractive and repulsive interactions, allow for one type of chain assembly only (see Figure 2c). This is of course a simplification, yet it is a first step towards understanding how self-propulsion affects polymerization. The parameter values used in the simulation are given in Table A1.

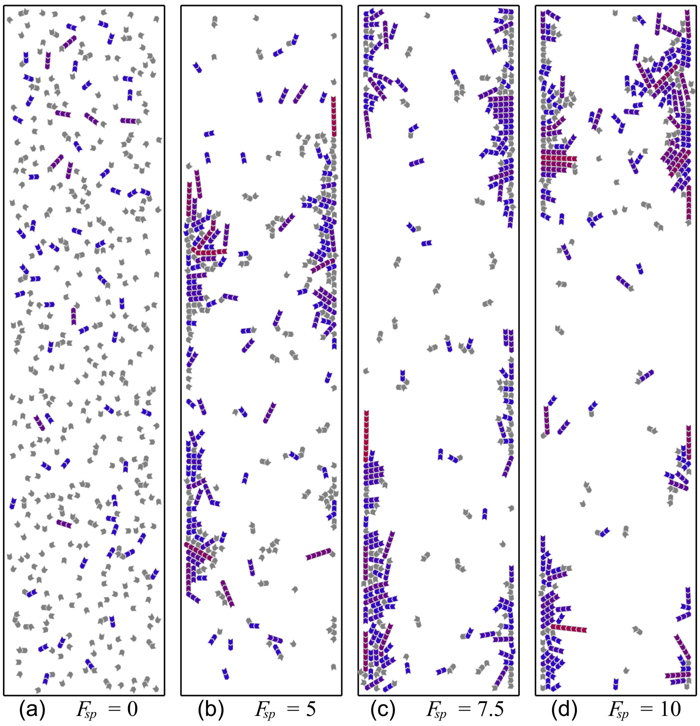

**Figure 5.** Effect of self-propulsion on the assembly of molecules within semi-periodic boundary conditions (channel), where the longest sides are reflecting boundaries and the shorter ones are periodic. All the snapshots correspond to temperature $T = 0.1$ and channel aspect ratio $R = 0.5$. For $F_{\mathrm{sp}} = 0$, i.e. when the motion of the molecules is driven just by thermal noise, only small polymers are formed. However, as the value of $F_{\mathrm{sp}}$ increases the length of the assembled polymers also increases. Note that in this case the polymers aggregate in the reflecting boundaries, allowing them to form even longer chains.

## 4. Results

For systems composed of $N = 500$ active molecules, numerical simulations were used to investigate two scenarios: (i) a system with periodic boundary conditions and (ii) a system with semi-periodic boundary conditions. In the first scenario, the molecules move inside a square box of sides $l$ in which the four boundaries are periodic. In the second, the molecules move inside a rectangle of sides $l_1$ and $l_2$, with $l_1 \leq l_2$. The two longest sides are reflecting walls whereas the two shortest sides are periodic, resembling a channel. We will refer to the second scenario as the *channel system*. The motivation for studying the channel system is based on the hypothesis that the formation of organic macro-molecules relevant to the origin of life may have occurred in micro-channels formed either in meteorites [32–35], or in confined micro-spaces of marine vent chimneys in which molecules are driven by thermal gradients [36]. Therefore, in this work numerical simulations were performed for different values of the thermal bath temperature $T$, the self-propulsion force $F_{sp}$. In addition, for the channel system, different values of the channel aspect ratio, defined as $R = l_1/l_2$, were considered.

Figure 4 shows different realizations for the system with periodic boundary conditions at constant temperature $T = 0.1$ and different values of the self-propulsion force $F_{sp}$. The case $F_{sp} = 0$ corresponds to spontaneous self-assembly, as it's driven only by thermal noise. It is apparent from Figure 4a that in this case, only very short polymers are formed while most of the molecules remain unbound. Contrary to this, for large values of the self-propulsion force (for instance $F_{sp} = 10$, Figure 4c), much longer polymers are created. Similar results are obtained for the channel system, as Figure 5 shows. Interestingly, for the channel system, most of the polymers tend to form and aggregate next to the reflecting walls, (see Figure 5). This is an unexpected result because there is no attractive force between

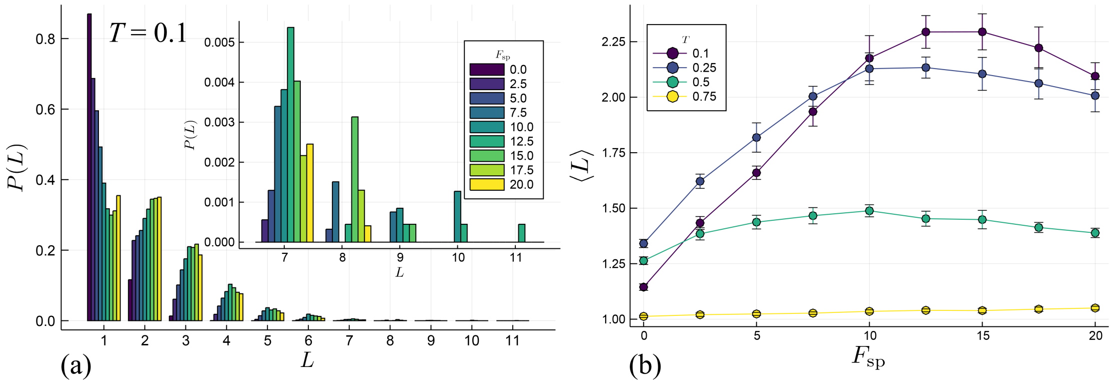

**Figure 6.** Results for the system with periodic boundary conditions. **(a)** Probability $P(L)$ that a polymer of length $L$ is created. Different colors correspond to different values of the self-propulsion force $F_{\text{sp}}$. All the simulations in this panel were computed at constant temperature $T = 0.1$. The inset shows a magnification of the tail of the distribution $P(L)$ in order to better appreciate the existence of long polymers. **(b)** Average chain length $\langle L \rangle$ as a function of the self-propelled force $F_{\text{sp}}$ for different temperatures values of the temperature $T$. Note that for lower temperatures, there is an optimal value of $F_{\text{sp}}$ at which $\langle L \rangle$ exhibits a maximum.

the walls of the channel and the molecules. The walls were implemented to make the molecules to elastically bounce back into the channel after a collision. A similar behavior was also observed in two different systems of active colloidal rods [37] and spheres [38].

To quantify the effect that self-propulsion has on the polymerization process, we calculated, for different values of the self-propulsion force $F_{sp}$ and temperature $T = 0.1$, the probability $P(L)$ that a polymer of length $L$ is created. The results are shown in Figure 6a. (It should be noted that $P(L)$ was computed once the system reached a stationary state). It is clear that by increasing the magnitude of $F_{sp}$, longer polymers are created. However, this behavior is not monotonic, as seen in Figure 6b, which shows the average polymer length $\langle L \rangle$ as a function of $F_{sp}$ for different temperatures. It is apparent from Figure 6b that at low temperatures there exists an optimal value of $F_{sp}$ for which $\langle L \rangle$ reaches a maximum. When $F_{sp}$ increases beyond this optimal value, the average polymer length $\langle L \rangle$ starts to decrease. This is due to the molecule-polymer and polymer-polymer collisions. When $F_{sp}$ is too large, these collisions are very energetic, disassembling the already formed polymers.

Similar results are presented in Figure 7 for the channel system with semi-periodic boundary conditions. The tail of the distribution $P(L)$ (inset in Figure 7a) reveals that much longer polymers are created in the channel system than in the system with fully periodic boundary conditions (inset in Figure 6a). This is due to the aggregation of molecules and polymers next to the reflecting channel walls, which decreases the velocity of the molecules and polymers preventing the occurrence of too energetic collisions which may disassemble the already formed polymers. In fact, from Figure 7b it can be observed that the average polymer length $\langle L \rangle$ for the channel system does not reach a maximum at any value of the self-propulsion force $F_{sp}$. Instead, $\langle L \rangle$ monotonously increases with $F_{sp}$ and then saturates.

## 5. Conclusion

We have presented a polymerization model of active self-propelled molecules. Our results show that self-propulsion considerably improves the polymerization of these molecules. As the magnitude of the self-propulsion force increases, longer polymers appear in comparison with the equilibrium case in which the spontaneous self-assembly is driven only by the Brownian motion of molecules as a result of the temperature of the thermal bath. When the molecules move in “free space” (fully periodic boundary conditions), there is an optimum value of the magnitude of the self-propulsion force for which the mean polymer length is maximum, and above which it decreases. This is due to the

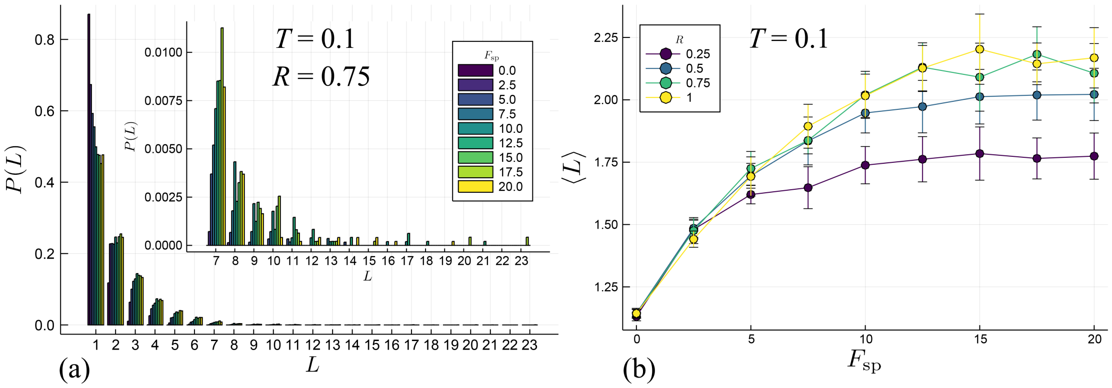

**Figure 7.** Results for the channel with semi-periodic boundary conditions. All the results presented in this figure were computed at constant temperature $T = 0.1$. **(a)** Probability $P(L)$ that a chain of length $L$ is formed for different values of the self-propulsion force $F_{\text{sp}}$ in a channel with an aspect-ratio $R = 0.75$. The inset shows a magnification of the tail of the distribution $P(L)$. Note that in this case, even longer polymers are formed with respect to the case with fully periodic boundary conditions depicted in Figure 6. **(b)** Average chain length $\langle L \rangle$ as a function of the self-propulsion force $F_{\text{sp}}$ for different values of the channel aspect-ratio $R$. Note that $\langle L \rangle$ first increases and then saturates as a function of $F_{\text{sp}}$.

competition between the bonding energy and the force exerted between molecules in collisions, where the repelling subunits interact. This competition takes place less often when the molecules move inside a channel with reflecting walls. In this case, the molecules and polymers tend to aggregate next to the walls, which decreases the velocity of both, molecules and polymers, preventing the occurrence, to some extent, of highly energetic collisions. Therefore, confinement inside reflecting boundaries also enhances the polymerization process.

Our results, and the ones obtained by other groups, show that self-propulsion acts as a catalyst in the assembly of ordered macroscopic structures from small molecules, let them be one-dimensional polymers, as in the model presented in this work, or capsides [11] or protein domains in a cell membrane [8]. Altogether, these results suggest that self-propulsion could have been an important mechanism for the formation of pre-biotic structures or the synthesis of nanometric structures. More theoretical and experimental work, however, is needed to shed light on this claim.

**Author Contributions:** All authors have read and agree to the published version of the manuscript. Conceptualization, M.A. and M.F.C.; methodology, M.A., M.F.C. and M.Z.; software, M.Z.; validation, M.A., M.F.C. and M.Z.; writing–original draft preparation, M.Z.; writing–review and editing, M.A., M.F.C. and M.Z.; funding acquisition, M.A. and M.F.C.

**Funding:** This research was partially funded by PAPIIT-UNAM grant number IN226917 and CONACyT through the Ph.D. Scholarship number 592408/307643 (M.Z.).

**Acknowledgments:** M.Z. acknowledges CONACyT for the Ph.D. Scholarship number 592408/307643. M.A. and M.F.C. acknowledge support and hospitality from the Earth-Life Science Institute of the Tokyo Institute of Technology. We also thank the High Performance Computing Facility at Centro de Ciencias de la Complejidad, UNAM, for support with the numerical simulations. A portion of this work (conceptualization, writing-editing and review) was conducted at the Center for Nanophase Materials Sciences, which is a DOE Office of Science User Facility.

**Conflicts of Interest:** The authors declare no conflict of interest. The funders had no role in the design of the study; in the collection, analyses, or interpretation of data; in the writing of the manuscript, or in the decision to publish the results.

## Appendix A. Parameter values used in the numerical simulations

Table A1 presents the values of the parameters used in the numerical simulations.

## References

1. Fox, G.E. Origin and evolution of the ribosome. *Cold Spring Harb. Perspec. Biol.* **2010**, 2, a003483.

Peer-reviewed version available at Entropy 2020, 22, 251; doi:10.3390/e22020251

| Active Colloids Self-assembly model | | |
|---|---|---|
| $N$ | Number of colloids | 512 |
| $N_s$ | Number of spherical subunits per colloid | 20 |
| $T$ | Temperature | $[0.1, 0.75]$ |
| $\sigma_s$ | Spherical subunit radius | 0.25 |
| $\gamma_r$ | Translational Friction | 250 |
| $D_r$ | Translational Diffusion Coefficient | $k_B T/\gamma_r$ |
| $\gamma_t$ | Rotational Friction | $D_r/k_b T$ |
| $D_t$ | Rotational Diffusion Coefficient | $3D_r/\sigma_s^2$ |
| $F_{\mathrm{sp}}$ | Self-propulsion force | $[0, 20]$ |
| $\Delta t$ | Integration step | $10^{-3}$ |
| $t_\infty$ | Number of time steps | $10^7$ |
| $R$ | Channel size ratio | $[0.25, 1]$ |
| $l$ | Size of the simulation cell | 135 |

**Table A1.** Parameters used in the numerical simulations. The molecules start at non overlapping random positions within the simulation cell.

2. Petrov, A.S. et. al. History of the ribosome and the origin of translation. *Proc. Natnl. Acad. Sci.* **2015**, 112, 15396-15401.
3. Monnard, A.P.; Appel, C.L.; Canavarioti, A.; Deamer, D.W. Influence of ionic inorganic solutes on self-assembly and polymerization processes related to early forms of life: implications for a prebiotic aqueous medium. *Astrobiology.* **2004**, 2, 139-152.
4. Lazcano, A. Prebiotic Evolution and Self-Assembly of Nucleic Acids. *ACS Nano* **2018**, 12, 9643-9647.
5. Cronin, L.; Walker, S.R. Beyond prebiotic chemestry. *Science.* **2016**, 352, 1174-1175.
6. Hud, V.N. Our Odyssey to Find a Plausible Prebiotic Path to RNA: The First Twenty Years. *SynLett.* **2017**, 28, 36-55.
7. Walker, S.R. Origins of life: a problem for physics,a key issues review. *Rep. Prog. Phys.* **2017**, 80, 092601.
8. John, K.; Bär, M. Alternative mechanisms of structuring biomembranes: Self-assembly versus self-organization. *Phys. Rev. Lett.* **2005**, 95, 198101.
9. Agerschou, E.D.; Mast, C.B.; Braun, D. Emergence of Life from Trapped Nucleotides? Non-Equilibrium Behavior of Oligonucleotides in Thermal Gradients. Synlett **2017**, 28, 56-63.
10. Wang, W.; Duan, W.; Ahmed, S.; Sen, A.; Mallouk, T.E. From One to Many: Dynamic Assembly and Collective Behavior of Self-Propelled Colloidal Motors. *Accounts of Chemical Research.* **2015**, 48, 1938-1946.
11. Mallory, S.A.; Cacciuto, A. Activity-assisted self-assembly of colloidal particles. *Phys. Rev. E.* **2016**. 94, 022607.
12. Whitesides, G.M; Grzybowski, B. Self-assembly at all scales. Science **2002**, 295, 5564, 2418-2421.
13. Kelly, R.E.A.; Lee, Y.J.; Kantorovich, L.N. Homopairing Possibilities of the DNA Base Adenine. *J. Phys. Chem. B.* **2005**, 109, 24, 11933-11939.
14. Otero, R.; Lukas, M.; Kelly, R.E.A.; et al. Elementary Structural Motifs in a Random Network of Cytosine Adsorbed on a Gold(111) Surface. *Science.* **2008**, 319, 312-315.
15. Bellini, T.; Zanchetta, G.; Fraccia, T.P. et al. Liquid crystal self-assembly of random-sequence DNA oligomers. *Proceedings of the National Academy of Sciences.* **2012**, 109, 1110-1115.
16. Cafferty, B.J.; Gállego, I.; Chen, M.C.; et al. Efficient Self-Assembly in Water of Long Noncovalent Polymers by Nucleobase Analogues. *J. Am. Chem. Soc.* **2013**, 135, 7, 2447-2450.
17. Wang, J.; Bonnesen, P.V.; Rangel, E.; et al. Supramolecular polymerization of a prebiotic nucleoside provides insights into the creation of sequence-controlled polymers. *Scientific Reports.* **2016**, 6, 18891.
18. Schellinck, J.; White, T. A review of attraction and repulsion models of aggregation: Methods, findings and a discussion of model validation. *Ecol. Modell.* **2011**, 222, 1897-1911.
19. Menzel, A.M. Tuned, driven, and active soft matter. *Physics Reports.* **2015**, 554, 1-46.
20. Bechinger, C.; Di Leonardo, R.; Löwen, H.; Reichhardt, C.; and Volpe, G.; Volpe, G. Active particles in complex and crowded environments. *Rev. Mod. Phys.* **2016**, 88, 045006.
21. Yeomans, J.M. Nature's engines: active matter. *Europhysics News.* **2017**, 48, 21-25.
22. Fialkowski, M.; Bishop, K.H.M.; Klajn, R.; et al. Principles and Implementations of Dissipative (Dynamic) Self-Assembly. *J. Phys. Chem. B.* **2006**, 110, 6, 2482-2496.

23. Vicsek, T.; Zafeiris, A. Collective Motion. *Physics Reports.* **2012**, 517, 71-140.
24. Attanasi, A.; Cavagna, A.; Del Castello, L.; et al. Information transfer and behavioural inertia in starling flocks. *Nature physics.* **2014**, 10, 615-698.
25. Andreas Zöttl and Holger Stark. Emergent behavior in active colloids. *J. Phys. Cond. Matt.* **2016**, 28, 253001.
26. Vicsek, T.; Czirók, A.; Ben-Jacob, E.; Cohen, I.; Shochet, O. Novel Type of Phase Transition in a System of Self-Driven Particles. *Phys. Rev. Lett.* **1995**, 75, 1226.
27. Schaller, V.; Weber, C.; Semmrich, C.; et al. Polar patterns of driven filaments. *Nature.* **2010**, 467, 73-77.
28. Huber, L.; Suzuki, R.; Krüger, T.; Frey, E.; Bausch, A.R. Emergence of coexisting ordered states in active matter systems. *Science*. **2018**, 361, 6399, 255-258.
29. Wensink, H.H.; Kantsler, V.; Goldstein, R.E.; Dunkel, J. Controlling active self-assembly through broken particle-shape symmetry. *Phys. Rev. E.* **2014**, 89, 010302.
30. Ilse, S.E.; Holm, C.; de Graaf, J. Surface roughness stabilizes the clustering of self-propelled triangles. *J. Chem. Phys.* **2016**, 145, 134904.
31. Wensink, H.H.; Löwen, H. Emergent states in dense systems of active rods: from swarming to turbulence. *J. Phys. Cond. Matt.* **2012**,24, 464130.
32. Ponnamperuma, C. Clay and the origin of life. *Origins of Life*. **1982**, 12, 9-40.
33. Pierazzo, E.; Chyba, C.F. Amino acid survival in large cometary impacts. *Meteoritics & Planetary Science*. **1999**, 6, 909-918.
34. Burton, A.S.; Stern, J.C.; Elsila, J.E. Understanding prebiotic chemistry through the analysis of extraterrestrial amino acids and nucleobases in meteorites. *Chem. Soc. Rev.*, **2012**, 41, 5459-5472.
35. Hashizume, H. Role of Clay Minerals in Chemical Evolution and the Origins of Life. In *Clay Minerals in Nature*; Valaskova, M., Martynková, G.S., Eds.; IntechOpen: London, U.K. **2012**, Chapter 10, 191-208.
36. Budin, I.; Szostak, J.W. Expanding Roles for Diverse Physical Phenomena During the Origin of Life. *Ann. Rev. Biophys.* **2010**, 39, 245-63.
37. Wensink, H.H. Löwen, H. Aggregation of self-propelled colloidal rods near confining walls. *Phys. Rev. E.* **2008**, 78, 031409.
38. Elgeti, J.; Gompper, G. Wall accumulation of self-propelled spheres. *Europhysics Letters*. **2013**, 101, 48003.
39. Reichhardt, C. Reichhardt, C.J.O. Active matter transport and jamming on disordered landscapes. *Phys. Rev. E.* **2014**. 90, 012701.
40. Ballerini, M.; Cabibbo, N.; Candelier, R.; et al. Interaction ruling animal collective behavior depends on topological rather than metric distance: Evidence from a field study. *Proceedings of the National Academy of Sciences*. **2008**, 105, 1232-1237.